



Original Article

NUP160 knockdown inhibits the progression of diabetic nephropathy *in vitro* and *in vivo*Jiyong Xie ^{a,d,**,1}, Zhi Chen ^{b,1}, Gang Yao ^c, Ying Yuan ^a, Wenjuan Yu ^c, Qiang Zhu ^{a,*}^a Department of Nephrology, Xinghua People's Hospital, Taizhou 225700, Jiangsu, China^b Department of Laboratory, Xinghua People's Hospital, Taizhou 225700, Jiangsu, China^c Department of Nephrology, Second Affiliated Hospital of Nanjing Medical University, Nanjing 210011, Jiangsu, China^d Kangda College of Nanjing Medical University, Lianyungang 222000, Jiangsu, China

ARTICLE INFO

Article history:

Received 15 April 2022

Received in revised form

20 May 2022

Accepted 26 May 2022

Keywords:

Diabetic nephropathy

HCG18

NUP160

Podocytes

ABSTRACT

Diabetic nephropathy (DN) is a severe diabetic complication and podocyte damage is a hallmark of DN. The Nucleoporin 160 (NUP160) gene was demonstrated to regulate cell proliferation and apoptosis in mouse podocytes. This study explored the possible role and mechanisms of NUP160 in high glucose-triggered podocyte injury. A rat model of DN was established by intraperitoneal injection of 60 mg/kg streptozotocin (STZ). Podocytes were treated with 33 mM high glucose. The effects of the Nup160 on DN and its mechanisms were assessed using MTT, flow cytometry, Western blot, ELISA, RT-qPCR, and luciferase reporter assays. The *in vivo* effects of NUP160 were analyzed by HE, PAS, and MASSON staining assays. The NUP160 level was significantly upregulated in podocytes treated with 33 mM high glucose. Functionally, NUP160 knockdown alleviated high glucose-induced apoptosis and inflammation in podocytes. Mechanistically, miR-495-3p directly targeted NUP160, and lncRNA HCG18 upregulated NUP160 by sponging miR-495-3p by acting as a ceRNA. Additionally, NUP160 overexpression reversed the effects of HCG18 knockdown in high glucose treated-podocytes. The *in vivo* assays indicated that NUP160 knockdown alleviated the symptoms of DN rats. NUP160 knockdown plays a key role in preventing the progression of DN, suggesting that targeting NUP160 may be a potential therapeutic strategy for DN treatment.

© 2022, The Japanese Society for Regenerative Medicine. Production and hosting by Elsevier B.V. This is an open access article under the CC BY-NC-ND license (<http://creativecommons.org/licenses/by-nc-nd/4.0/>).

1. Introduction

Diabetic nephropathy (DN) is a severe diabetic complication, with chronic hyperglycemia, proteinuria, and edema as the main manifestations [1]. Typical pathological features include tubulo-interstitial fibrosis and glomerulosclerosis resulting from renal tubulo-interstitium, increased deposition of extracellular matrix

Abbreviations: DN, diabetic nephropathy; NUP160, Nucleoporin 160; STZ, streptozotocin; ECM, extracellular matrix; NPC, nuclear pore complex; ELISA, Enzyme-linked immunosorbent assay; HE, Hematoxylin-eosin; ceRNAs, competitive endogenous RNAs; miRNAs, MicroRNAs.

* Corresponding author: Xinghua People's Hospital, No. 419, Yingwu South Road, Xinghua, Taizhou, Jiangsu, China.

** Corresponding author.

E-mail addresses: xiejiayong2019@sina.com (J. Xie), zhuqiang4721@sina.com (Q. Zhu).

Peer review under responsibility of the Japanese Society for Regenerative Medicine.

¹ These authors contributed equally to this work.

<https://doi.org/10.1016/j.reth.2022.05.011>

2352-3204/© 2022, The Japanese Society for Regenerative Medicine. Production and hosting by Elsevier B.V. This is an open access article under the CC BY-NC-ND license (<http://creativecommons.org/licenses/by-nc-nd/4.0/>).

(ECM) in mesangium, and thickening of glomerular basement membranes [2]. The pathogenesis of DN is complicated, including hyperglycemia, hypertension, and abnormal renal hemodynamics and metabolism of vasoactive substances [3]. Although established therapeutic strategies, such as appropriate blood glucose control, blood pressure control with renin-angiotensin system blockade, and lipid lowering with statins, are used to treat diabetes, the contribution of diabetic end-stage kidney disease to the total number of cases requiring hemodialysis has increased tremendously in the past decades [4]. Therefore, slowing renal function decline is one of the main areas of focus in DN research, and novel strategies are urgently needed to prevent diabetic kidney disease progression.

Podocytes are differentiated postmitotic cells located outside the basement membrane of glomerular capillaries and are involved in the constitution of the glomerular hemofiltration barrier [5]. Podocyte injury is an early indicator of many glomerular diseases, which leads to glomerular filtration barrier dysfunction, thus playing an important role in DN development [6,7]. Oxidative stress

activated by hyperglycemia and subsequent inflammatory response are key components in DN pathogenesis [8,9], which can induce the activation of apoptotic signaling that is involved in DN progression [10]. Moreover, excessive release of inflammatory cytokines in DN further accelerates oxidative stress, and as a result, intensified renal injury through forming a vicious cycle [11,12]. Increasing evidence demonstrates that apoptosis and inflammation can be provoked under high glucose conditions, and the mechanisms of high glucose-induced injury are further complicated due to the interaction of these two pathways [13]. Therefore, investigating the molecular mechanisms of suppressing apoptosis and inflammation may be a therapeutic pool for DN treatment.

As genetics and molecular biology develop, genetic factors have been increasingly highlighted in the course of diseases. Many genes encoding nucleoporins, such as NUP93, NUP107 and NUP205 were reported to participate in the pathogenesis of nephrotic syndrome [14–16]. The Nucleoporin 160 (NUP160) gene is located in chromosome 11p, encoding nucleoporin 160 kDa, which is a component of the Nup107–160 complex required for early stages of nuclear pore complex (NPC) assembly [17]. Within a nonconsanguineous Chinese family two siblings, a brother with steroid-resistant nephrotic syndrome and a sister with proteinuria, were both found to carry NUP160^{E803K} and NUP160^{R9103} compound-heterozygous mutations [18]. It has been reported that NUP160 depletion restrains cell proliferation, promotes apoptosis and migration in mouse podocytes [19]. Moreover, our previous study demonstrated that NUP160 is upregulated in high glucose (HG)-treated renal tubular cells and its downregulation inhibits inflammation and fibrosis [20]. However, the role of NUP160 in high glucose-treated podocytes has not been investigated.

Long non-coding RNAs (lncRNAs) are noncoding RNAs with a length >200 nucleotides, and microRNA (miRNAs/miRs) are a class of noncoding single-stranded RNA molecules with a length of ~22 nucleotides encoded by endogenous genes. lncRNAs play crucial roles in regulating various biological processes including DN by functioning as a competitive endogenous RNA (ceRNA) by competitively binding to miRNAs with downstream targets [21,22]. Our bioinformatics analysis revealed that NUP160 might act as a target of miR-495-3p, and lncRNA HLA complex group 18 (HCG18) harbors predicted binding sites of miR-495-3p. It has been reported that HCG18 is implicated in biological processes of various diseases, such as acute renal injury [23], cancers [24], myasthenia gravis [25], and osteoporosis [26]. Importantly, HCG18 is found highly expressed in patients with non-alcoholic fatty liver disease and participates in the regulation of insulin resistance [27]. Additionally, HCG18 has been demonstrated to promote M1 macrophage polarization and facilitate the progression of diabetic peripheral neuropathy, a main complication of type 2 diabetes mellitus [28]. It is highly suggestive of the various functions of HCG18, which provides more possibilities for the research of HCG18 in DN. In this study, we established a rat model of DN by intraperitoneal injection of streptozotocin (STZ) and treated podocytes with high glucose. We hypothesized that HCG18 might function as a ceRNA by sponging miR-495-3p to upregulate NUP160 expression, regulating high glucose-induced apoptosis and inflammation in podocytes. This study aimed to explore the pathogenesis of DN and offer a theoretical basis for DN treatment.

2. Materials and methods

2.1. Podocyte culture and treatment

The conditionally immortalized human podocyte cell line (cat. no. BNCC340460; Bena Culture Collection, Suzhou, China) was cultured in Dulbecco's modified Eagle's medium (cat. no.

SH30022.01B; HyClone, Logan, UT, USA) containing 10% FBS (cat. no. SH30070.03; HyClone), 0.5% penicillin/streptomycin (cat. no. 15140122; Gibco-BRL, Grand Island, NY, USA), and 5.6 mM glucose at 37 °C with 5% CO₂. For high-glucose treatment, cells were incubated in medium without serum for 12 h, followed by treatment with 33 mM high glucose for 48 h. 5.6 mM glucose (Control) and 5.6 mM glucose + 27.4 mM mannitol (Mannitol; cat. no. M9647; Sigma–Aldrich, St. Louis, MO, USA) were used as controls.

2.2. Transfection

NUP160 overexpression vector (NUP160), the empty vector (vector), miR-495-3p mimics (miR-495-3p), the control (NC mimics), short hairpin RNA (shRNA) of NUP160/HCG18 (sh-NUP160/sh-HCG18), and the control shRNA (sh-NC) were obtained from GenePharma (Shanghai, China). Transfection was performed using Lipofectamine 2000 (cat. no.11668; Invitrogen, Carlsbad, CA, USA) when cell confluence reached 70%.

2.3. RT-qPCR

RNA from renal tissues and podocytes was extracted utilizing TRIzol reagent (cat. no. 15596026; Invitrogen). The miRNA was extracted using the mirPremier microRNA Isolation Kit (cat. no. SNC10; Sigma–Aldrich). The extracted RNA (1 µg) was used to yield cDNA using the SuperScript Reverse Transcription Kit (cat. no. 4368813; Thermo Fisher Scientific, Waltham, MA, USA). The quantitative PCR was conducted using the SYBR Green PCR Kit (cat. no. RR086A; TaKaRa, Dalian, China) and gene-specific primers based on 7900HT Fast Real-Time PCR System (Applied Biosystems, Foster City, CA, USA). The miRNA expression was measured with the TaqMan MicroRNA Assay Kit (cat. no. 4427975; Thermo Fisher Scientific). The 2^{-ΔΔCt} method was used for the calculation of gene expression, normalizing genes to GAPDH and U6. The primer sequences were taken from the public database and were synthesized by Sangon Biological Engineering Co., Ltd (Shanghai, China). PCR primers are listed as follows: NUP160, forward: 5'-AGTATCAGGGGTGACCACT-3', reverse: 5'-TTCCAGCAGTAAGCCGAAGG-3'; HCG18, forward: 5'-TGAAGTCGACGAGAGGAC-3', reverse: 5'-ACTAGTCGA-GAGTGAGGTGC-3'; miR-495-3p, forward: 5'-ACACTCCAGCTGG-GAAACAACATGGTGCA-3', reverse: 5'-TGGTGTCTGGAGTTCG-3'; U6, forward: 5'-CTCGCTCGGCAGCACA-3', reverse: 5'-AACGCTT-CACGAATTTGCGT-3', GAPDH, forward: 5'-CAAGTCATCCATGA-CAACTTTC-3', reverse: 5'-GTCCACCACCCTGTTGCTGTAG-3'.

2.4. Western blot

Total protein from podocytes was extracted and the concentration was measured by the bicinchoninic acid kit (cat. no. P0010S; Beyotime, Shanghai, China). Protein was subjected to 10% SDS-PAGE, and then transferred to membranes (cat. no. IPVH00010; Millipore, Billerica, MA, USA). Membranes were blocked in 5% skimmed milk for 1 h at 37 °C, and then incubated with primary antibodies Bax (ab182734, Abcam), Cleaved caspase-3 (ab32042), Cleaved caspase-9 (ab2324), NUP160 (ab73293), and GAPDH (ab181603) at 4 °C overnight. After washing, the membranes were probed with a secondary HRP-conjugated antibody (cat. no. 7074; Cell Signaling Technology, Inc., MA, USA) for 2 h at 37 °C. Afterwards, the enhanced chemiluminescence reagent (cat. no. PE0010-100; Beijing Solarbio, China) was used to visualize the immunoreactive bands on the blots.

2.5. MTT

Podocytes (1 × 10⁴ cells) were seeded in 96-well plates for 24 h. Next, 10 µl MTT solution (5 mg/ml; cat. no. M-0283;

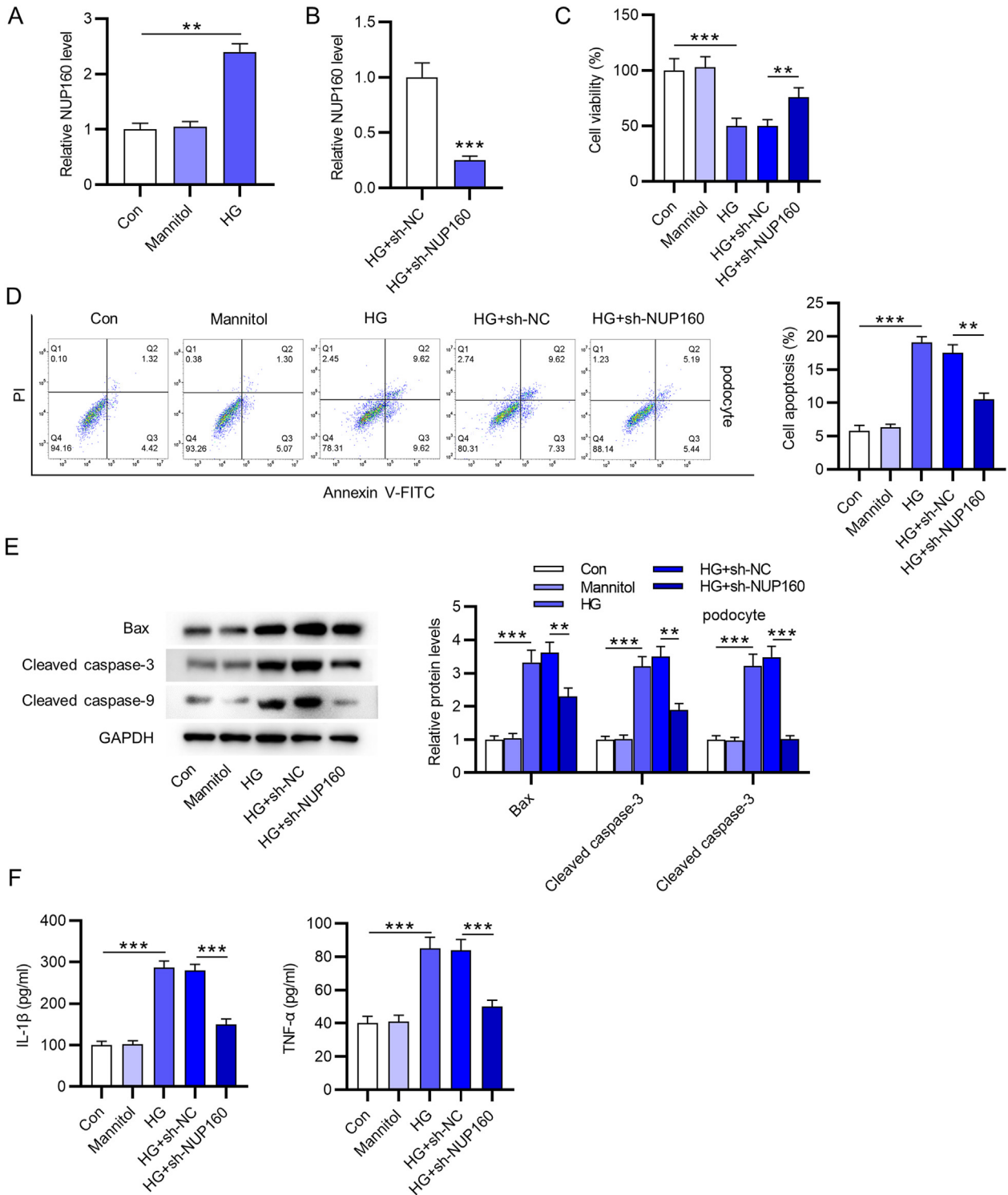


Fig. 1. NUP160 knockdown alleviates high glucose-induced injury in podocytes. (A) The NUP160 level in high glucose-treated podocytes was analyzed by RT-qPCR. (B) The sh-NUP160 transfection efficiency in high glucose-treated podocytes was analyzed by RT-qPCR. (C) Cell growth in high glucose-treated podocytes upon NUP160 knockdown was measured by MTT assay. (D) Cell apoptosis in high glucose-treated podocytes upon NUP160 knockdown was measured by flow cytometry analysis. (E) Apoptosis protein levels in high glucose-treated podocytes upon NUP160 knockdown were assessed by Western blot. (F) The inflammatory cytokines in high glucose-treated podocytes upon NUP160 knockdown were analyzed by ELISA. ***p* < 0.01, ****p* < 0.001.

Sigma–Aldrich) was added to plates for 4 h of incubation at 37 °C. After the supernatant was removed, 150 μl dimethyl sulfoxide (cat. no. D2650; Sigma–Aldrich) was added to dissolve the formazan in cells. After 10 min, absorbance was detected with a Bio–Rad Model 550 microplate reader (Bio–Rad Laboratories Inc., Hercules, CA, USA). The cell viability histogram was plotted based on this.

2.6. Apoptosis analysis

The Annexin V-FITC/PI Kit (cat. no. 40302ES20; YEASEN, Shanghai, China) was utilized to detect cell apoptosis. Briefly, podocytes (1×10^6 cells) were centrifuged, suspended, and stained with 5 μl Annexin V-FITC for 10 min in the dark, and then added

with 5 μ l PI for 5 min in the dark at 25 °C. Cell apoptosis was monitored using BD FACSCalibur Flow Cytometer (BD Biosciences, San Jose, CA, USA).

2.7. Enzyme-linked immunosorbent assay (ELISA)

Podocytes were homogenized, after which homogenates were centrifuged at 9000 g for 30 min at 4 °C. The levels of interleukin (IL)-1 β (ab197742) and tumor necrosis factor (TNF)- α (ab208348) in the supernatant were measured using the ELISA Kits (Abcam) according to the protocols.

2.8. Luciferase reporter assay

The binding site of NUP160/HCG18 and miR-495-3p was predicted at the starBase website (<http://starbase.sysu.edu.cn/>) [29]. Wild type HCG18 or NUP160 was constructed, and their targeted sequence was mutated to generate mutant HCG18 or NUP160. These segments were inserted into the pmirGLO reporter vector (cat. no. E1330; Promega, Madison WI, USA). Recombinant vectors including HCG18-WT/Mut and NUP160-WT/Mut were co-transfected into podocytes with miR-495-3p mimics or NC mimics, respectively, for 48 h. Luciferase activity was evaluated using the luciferase detection kits (cat. no. RG005; Beyotime).

2.9. Animal models

Animal experiments were performed according to the Guide to the Management and Use of Laboratory Animals and were approved by the Institutional Animal Care and Use Committee of Xinghua People's Hospital. Twenty-four male SD rats (200–250 g) were

purchased from Vital River Co. Ltd. (Beijing, China). All rats received one week of acclimation in a pathogen-free environment with free access to water and food. They were divided into control + AAV-sh-NC group, control + AAV-sh-NUP160 group, STZ + AAV-sh-NC, and STZ + AAV-sh-NUP160 group with 6 rats in each group. Next, rats were fasted overnight and received an intraperitoneal streptozotocin (STZ) injection (60 mg/kg; cat. no. S0130; Sigma–Aldrich) in 0.01M citrate buffer for 5 consecutive days. Rats in the control groups were injected with the same amount of citrate buffer. After 48 h, a blood glucose level of ≥ 16.7 mM indicated a successful establishment of DN model. At 2 weeks after STZ injection, AAV-sh-NC or AAV-sh-NUP160 constructed by HanBio (Shanghai, China) was intravenously injected into the tail vein of rats (titer: 1×10^{11} viral genomes per rat, at a 3-day interval for 8 weeks). Rats were fasted for 6 h before they were euthanized. Kidneys were removed, with one part for RNA measurement and the other part for histological evaluation.

2.10. 20Hematoxylin-eosin (HE), masson and PAS staining

As previously described [30,31], kidney tissues were fixed in 4% paraformaldehyde (cat. no. P6148-100G; Sigma–Aldrich), embedded in paraffin, and cut into 3- μ m sections. The sections were then subjected to HE staining for histological evaluation. Masson and PAS staining was performed to assess renal fibrosis. Glomerular, tubular morphology and collagen were examined using a microscope (BX53; Olympus, Tokyo, Japan).

2.11. Statistical analysis

All assays were performed three times or more. Statistical analysis was conducted using SPSS version 21.0 software (IBM SPSS,

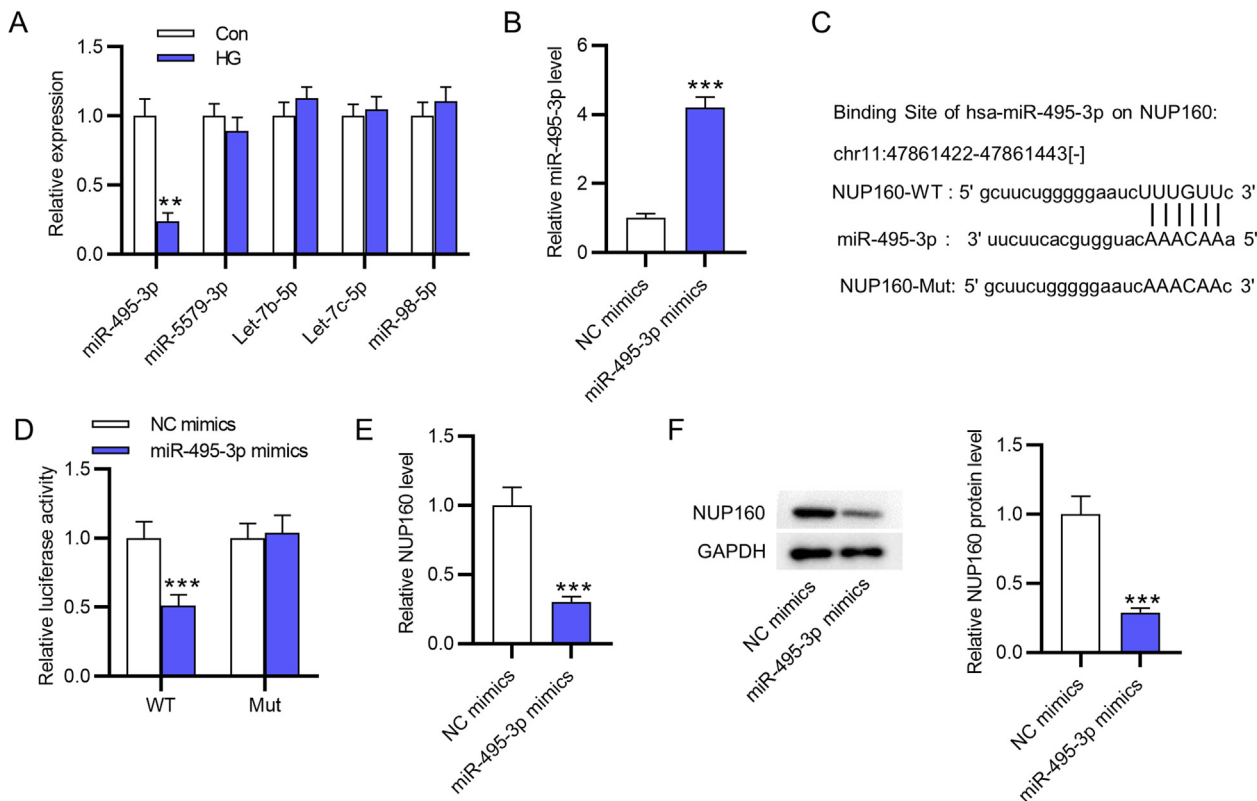


Fig. 2. MiR-495-3p directly targets NUP160. (A) The expression of miRNAs in high glucose-treated podocytes was measured by RT-qPCR. (B) The transfection efficiency of miR-495-3p mimics in podocytes was analyzed by RT-qPCR. (C) A binding site between NUP160 and miR-495-3p. (D) Luciferase reporter assay was performed to detect luciferase activity in podocytes transfected with the indicated plasmids. (E) The NUP160 mRNA level in podocytes transfected with miR-495-3p mimics was analyzed by RT-qPCR. (F) The NUP160 protein level in podocytes transfected with miR-495-3p mimics analyzed by RT-qPCR. **p < 0.01, ***p < 0.001.

Chicago, IL, USA). Data are expressed as the mean ± SD. Statistical evaluation was carried out using unpaired t-test or one-way ANOVA. Value of *p* < 0.05 was statistically significant.

3. Results

3.1. NUP160 knockdown alleviates high glucose-induced injury in podocytes

First, podocytes were treated with 33 mM glucose or an equal amount of mannitol for 48 h. RT-qPCR showed that the NUP160 level was significantly upregulated in high glucose-treated podocytes (Fig. 1A). To explore whether NUP160 affects podocytes *in vitro*, NUP160 was then knocked down by sh-NUP160 transfection in high glucose-treated podocytes (Fig. 1B). MTT was used to assess podocyte viability upon NUP160 downregulation. Data showed that NUP160 downregulation restored cell viability inhibited by high glucose in podocytes (Fig. 1C). Analysis of flow cytometry suggested that high glucose markedly accelerated the apoptosis of podocytes, while this effect was eliminated after NUP160 knockdown (Fig. 1D). Consistent with the results of flow cytometry, Western blot demonstrated that the levels of Bax, cleaved caspase-3, and cleaved caspase-9 were elevated in high glucose-treated podocytes compared to control, while NUP160 knockdown reversed these results (Fig. 1E). Furthermore, we used ELISA to examine whether NUP160 affects inflammation in podocytes after high glucose stimulation. As shown, the concentration of IL-1β and TNF-α was increased in the supernatant of podocytes treated with high glucose, and downregulation of NUP160 significantly suppressed the release of these cytokines (Fig. 1F). These findings confirmed that downregulation of NUP160 attenuates high glucose-induced podocyte injury *in vitro*.

3.2. MiR-495-3p directly targets NUP160

To investigate the possible mechanism of NUP160 in DN, the upstream miRNAs of NUP160 were predicted using starBase database. Five miRNAs (miR-495-3p, miR-5579-3p, let-7b-5p, let-7c-5p, and miR-98-5p) were selected and their expression levels in high glucose-treated podocytes was determined. We found that only miR-495-3p was significantly upregulated among these miRNAs (Fig. 2A). Next, the miR-495-3p level was upregulated by transfection with miR-495-3p mimics in high glucose-treated podocytes (Fig. 2B). Fig. 2C shows that NUP160 3'UTR contains a binding site for miR-495-3p. Wild type (WT) NUP160 3'UTR and Mutant (Mut) NUP160 3'UTR (without the requisite miR-495-3p binding sequence) vectors were transfected into podocytes along with miR-495-3p mimics. A decreased luciferase activity in cells containing WT-NUP160 3'UTR and miR-495-3p mimics was found, while there was no change in the luciferase activity when the binding site was mutant (Fig. 2D). Additionally, the expression of NUP160 mRNA and protein was reduced in podocytes transfected with miR-495-3p mimics (Fig. 2E and F). These data verified that NUP160 could bind to miR-495-3p.

3.3. HCG18 upregulates NUP160 by sponging miR-495-3p

LncRNAs could regulate biological processes via competitively binding to miRNAs as competitive endogenous RNAs (ceRNAs). We found 10 lncRNAs (AC051619.8, NEAT1, AC006511.3, ARHGAP27P1, NORAD, AC005538.2, MEG8, NEAT1, AC023509.1, and HCG18) that may bind to miR-495-3p at the starBase website and analyzed their expression levels in high glucose-treated podocytes. The results indicated that high glucose significantly increased the expression of HCG18 in podocytes, while the other lncRNAs had no

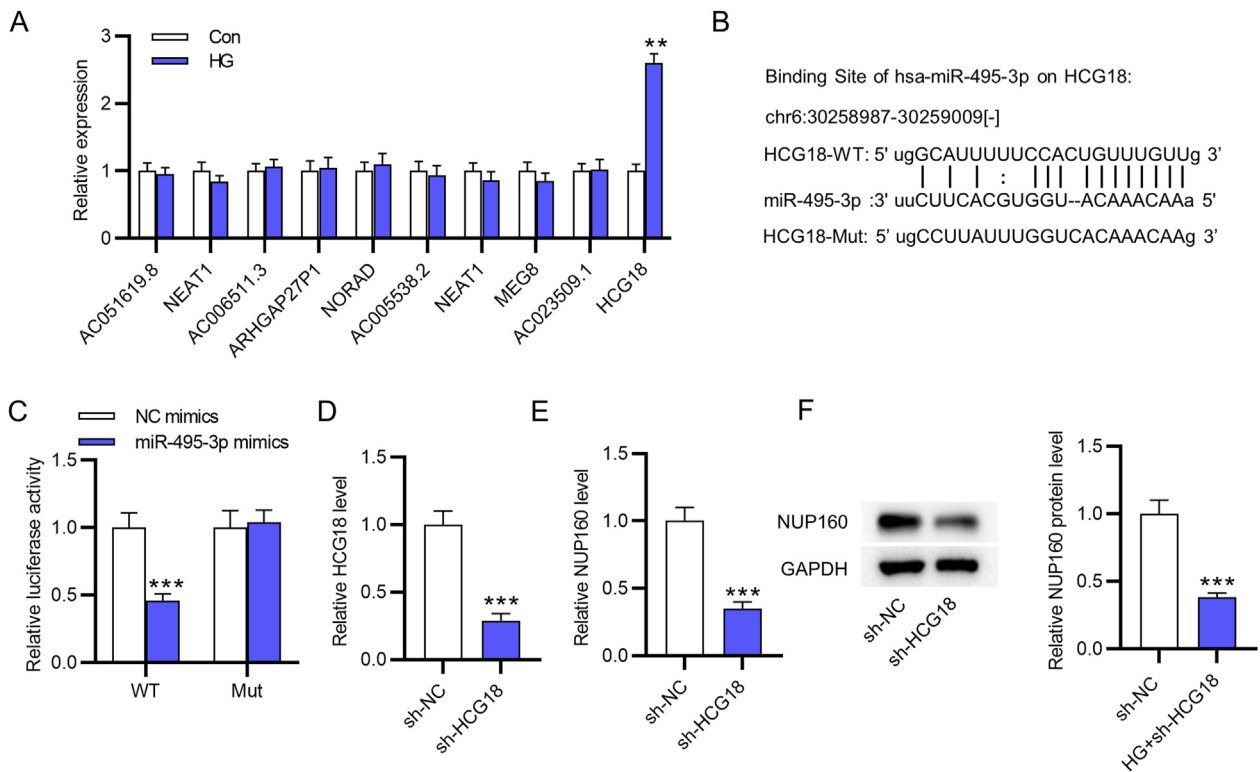


Fig. 3. HCG18 upregulates NUP160 by sponging miR-495-3p. (A) The expression of lncRNAs in high glucose-treated podocytes was determined by RT-qPCR. (B) A binding site between HCG18 and miR-495-3p. (C) Luciferase reporter assay was performed to detect luciferase activity in podocytes transfected with the indicated plasmids. (D) The sh-HCG18 transfection efficiency in podocytes was analyzed by RT-qPCR. (E) The NUP160 mRNA level in podocytes transfected with HCG18 was determined by RT-qPCR. (F) The NUP160 protein level in podocytes transfected with HCG18 was determined by Western blot. ***p* < 0.01, ****p* < 0.001.

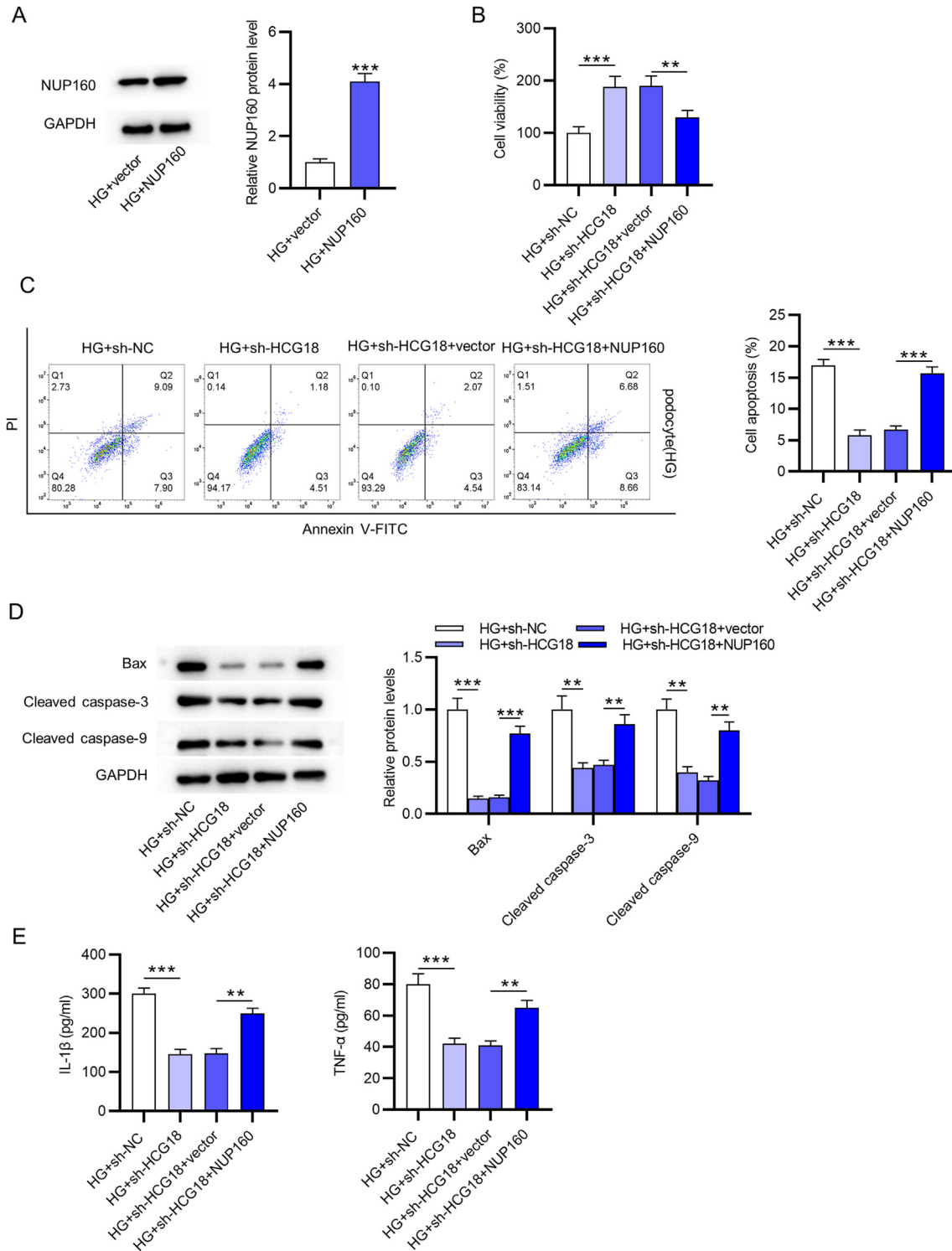


Fig. 4. NUP160 overexpression reverses the effect of HCG18 knockdown in high glucose treated-podocytes. (A) The NUP160 transfection efficiency in high glucose-treated podocytes was measured by Western blot. (B) Cell growth in high glucose-treated podocytes was assessed by MTT assay. (C) Cell apoptosis in high glucose-treated podocytes was evaluated by flow cytometry analysis. (D) Apoptosis protein levels in high glucose-treated podocytes were measured by Western blot. (E) The inflammatory cytokines in high glucose-treated podocytes were detected by ELISA. ****p* < 0.01, *****p* < 0.001.

significant change in the expression levels (Fig. 3A). Considering the participant of HCG18 in diabetes-associated disease, we selected HCG18 for the subsequent investigations. A binding site between HCG18 and miR-495-3p is presented (Fig. 3B). Luciferase reporter assay confirmed the binding of HCG18 to miR-495-3p (Fig. 3C). High glucose treated-podocytes were then transfected

with sh-HCG18, and RT-qPCR confirmed the knockdown efficiency (Fig. 3D). Analyses of RT-qPCR and Western blot revealed that HCG18 upregulated the expression of NUP160 mRNA and protein in podocytes (Fig. 3E and F). Overall, HCG18 acts as a ceRNA to upregulate NUP160 expression by competitively binding to miR-495-3p.

3.4. NUP160 overexpression reverses the effect of HCG18 knockdown in high glucose treated-podocytes

Next, we examined the regulatory role of the HCG18/miR-495-3p/NUP160 axis in high glucose-induced podocyte injury. Western blot indicated that the protein level of NUP160 in high glucose treated-podocytes was increased after transfection with NUP160 (Fig. 4A). As the MTT results revealed, NUP160 overexpression inhibited the cell viability promoted by sh-HCG18 in high glucose-treated podocytes (Fig. 4B). Additionally, HCG18 knockdown significantly suppressed the apoptosis of high glucose-treated podocytes, while this effect was attenuated after overexpressing NUP160 (Fig. 4C). NUP160 overexpression further restored the levels Bax, cleaved caspase-3, and cleaved caspase-9 in high glucose-treated podocytes transfected with sh-HCG18 (Fig. 4D). Moreover, the effects of HCG18 knockdown on the concentration of pro-inflammatory cytokines were reversed by NUP160 overexpression (Fig. 4E). These findings showed that HCG18 overexpression aggravates high glucose-induced podocyte injury by upregulating NUP160 expression.

3.5. NUP160 knockdown alleviates the symptoms of DN rats

Intraperitoneal injection of STZ was performed to establish a rat model of DN. The renal pathology of rats was observed using HE, PAS, and Masson staining assays. In Fig. 5A, rats in the control group showed normal morphology with tightly arranged renal tubules and regular glomerulus and capillary lumen. Rats in the AAV-sh-NC STZ group showed significantly thickened basement membrane, mesangial matrix hyperplasia, hyaline change in glomerular capillary lumen, and renal tubule and interstitial fibrosis. The injection of AAV-sh-NUP160 significantly restored these pathological changes in rats with STZ.

4. Discussion

Podocyte injury is aggravated due to apoptosis and inflammation under high glucose conditions. A high glucose-induced model of podocyte injury was widely used to mimic DN *in vitro* [32,33]. A study showed that NUP160 knockdown inhibits cell proliferation, induces apoptosis, autophagy, and cell migration, and alters both the expression and localization of podocyte associated molecules in mouse podocytes [19]. In this study, we found that NUP160 expression was upregulated in podocytes after high glucose treatment. Our findings further revealed that NUP160 knockdown alleviated high glucose-induced apoptosis and inflammation in podocytes. This suggests that the role of NUP160 depends on the cellular and molecular context. Our previously published report demonstrated that NUP160 expression is upregulated in DN mice. Depletion of NUP160 inhibited inflammation and fibrosis in HG-treated kidney tubular epithelial cells and restored pathological changes in STZ-induced DN mice by inactivating nuclear factor (NF)-κB signaling [20]. In this research, NUP160 knockdown was shown to restore the pathological changes of STZ-subjected rats. Therefore, NUP160 knockdown plays a key role in inhibiting the progression of DN.

Emerging studies have suggested that podocyte apoptosis is a critical indicator in the pathophysiology of DN [34,35]. Therefore, the investigation of preventing podocyte apoptosis may be a targeted intervention to impede DN progression [36]. Here, we found a significant reduction in podocyte survival after high glucose stimulation, while NUP160 knockdown antagonized these effects. Meanwhile, podocyte apoptosis was aggravated by high glucose treatment, accompanied by upregulation of Bax, cleaved caspase-3, and cleaved caspase-9. However, NUP160 knockdown resulted in a marked inhibition of high glucose-induced apoptosis, suggesting NUP160 knockdown protects podocytes against apoptosis. Evidence

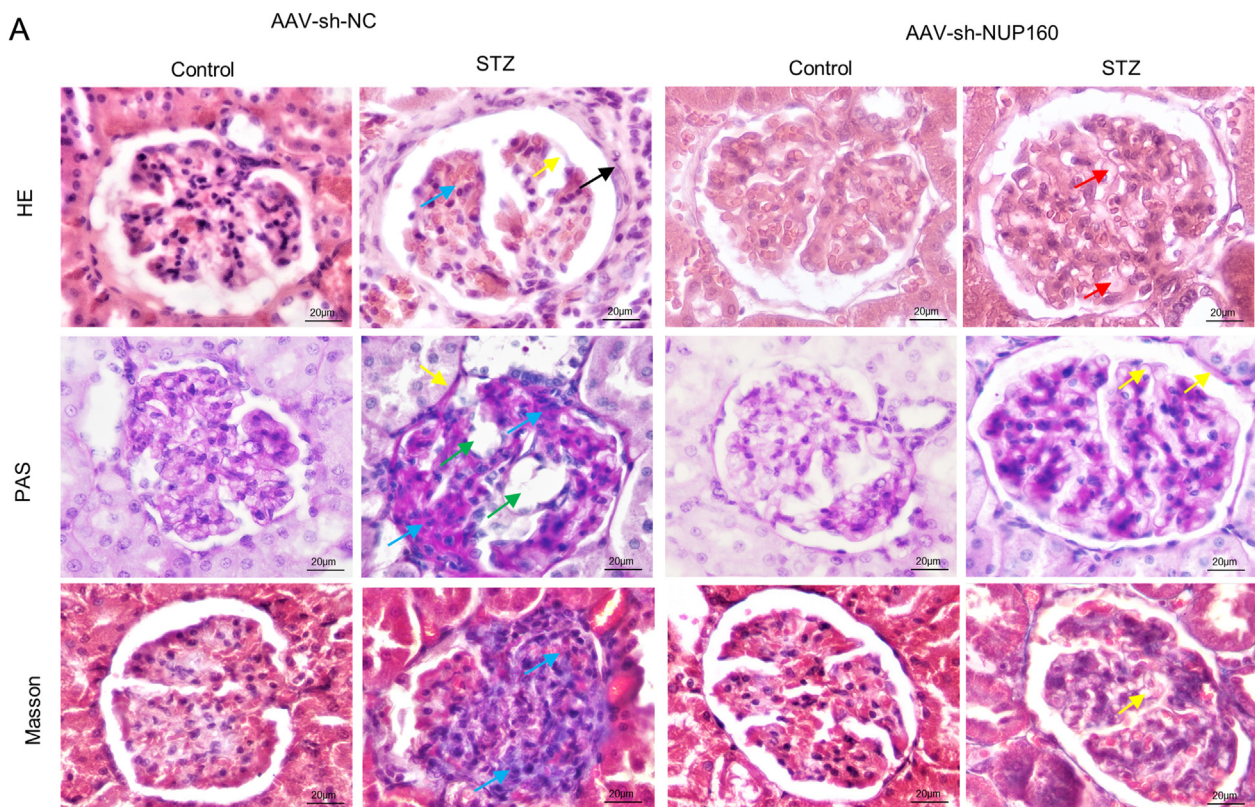


Fig. 5. NUP160 knockdown alleviates the symptoms of DN rats. (A) The renal pathology of rats was observed using HE, PAS, and Masson staining assays. N = 12.

has shown the key role of inflammation in DN [37,38]. It has been reported that uncontrolled diabetes can lead to generation of multiple types of inflammatory mediators [9]. In this investigation, we detected that high glucose notably increased the levels of IL-1 β and TNF- α in podocytes, and NUP160 knockdown alleviated production of these cytokines, demonstrating that NUP160 knockdown exerts an anti-inflammatory effect in high glucose-treated podocytes. Overall, these findings indicated that NUP160 knockdown alleviates podocyte injury induced by high glucose.

MicroRNAs (miRNAs) are single-stranded noncoding RNAs that are 21–24 nucleotides and function as major regulators of gene expression by binding to mRNA 3'UTR [39]. Recently, the involvement of miRNAs in the pathology of renal diseases has been widely reported [40,41]. Additionally, emerging reports have revealed that miRNAs could act as potential therapeutic targets in DN [42]. For example, miR-770-5p aggravates podocyte apoptosis and inflammation in DN by inhibition of metalloproteinase 3 [43]. MiR-15b-5p attenuates high glucose-triggered podocyte apoptosis and oxidative stress by targeting Semaphorin 3A [44]. As previously reported, miR-495-3p exert a pro-fibrotic effect and thus induces mitochondrial damage associated with renal fibrosis [45]. In addition, miR-495-3p was reported to promote cell apoptosis in several cancers [46,47]. In the current study, miR-495-3p was observed to be downregulated under high glucose conditions. A predicted binding site of NUP160 in miR-495-3p was predicted using bioinformatical tools. Then, the binding of NUP160 to miR-495-3p was confirmed. Furthermore, miR-495-3p negatively modulated NUP160 expression at mRNA and protein levels. Thus, we concluded that NUP160 is a direct target of miR-495-3p. However, the functional role of miR-495-3p in high glucose-induced podocyte injury should be verified in future investigations.

The ceRNA plays an essential role in the precise control of target gene expression [48]. Dysregulation of many lncRNAs has been shown to be related to DN development. For example, lncRNA NONHSAG053901 facilitates renal inflammation and fibrosis in DN by binding to early growth response-1 [49]. lncRNA XIST protects podocytes against high glucose-triggered injury in DN [50]. A study demonstrated that the HCG18 level is increased in high glucose-induced Raw 264.7 macrophages and peripheral nervous tissues of diabetic peripheral neuropathy and its overexpression upregulates the expression of IL-6, IL-1 β and TNF α [28]. Consistent with these results, here, HCG18 was found to be upregulated in high glucose-treated podocytes. We further verified the interaction between HCG18 and miR-495-3p. Furthermore, HCG18 positively modulated NUP160 expression at mRNA and protein levels. Functionally, HCG18 knockdown attenuated podocyte apoptosis and inflammation induced by high glucose, while overexpression of NUP160 reversed these effects.

5. Conclusion

In summary, our findings show that inhibition of NUP160 could attenuate high glucose-induced podocyte injury *in vitro* and alleviate the symptoms of DN rats *in vivo*. Additionally, HCG18 positively regulates NUP160 by sponging miR-495-3p. This study may provide a theoretical basis for the exploration of the mechanisms in DN, suggesting that targeting NUP160 may be a potential therapeutic strategy for DN treatment.

Ethics approval and consent to participate

Animal experiments strictly followed the Guide to the Management and Use of Laboratory Animals and were approved by the Institutional Animal Care and Use Committee of Xinghua People's Hospital (Jiangsu, China).

Consent for publication

Not applicable.

Availability of data and material

The datasets used during the current study are available from the corresponding author on reasonable request.

Authors' contributions

Jiayong Xie and Zhi Chen conceived and designed the experiments. Jiayong Xie, Zhi Chen, Gang Yao, Ying Yuan, Wenjuan Yu and Qiang Zhu carried out the experiments. Jiayong Xie, Zhi Chen, and Qiang Zhu analyzed the data. Jiayong Xie, Zhi Chen, and Qiang Zhu drafted the manuscript. All authors agreed to be accountable for all aspects of the work. All authors have read and approved the final manuscript.

Funding

This work supported by Taizhou Science and Technology Support Plan (Social Development) Project (No: SSF20200028), Scientific Research and Development fund of Kangda College of Nanjing Medical University (NO: KD2021KYJJZD062).

Declaration of competing interest

The authors declare that they have no competing interests.

Acknowledgement

Not applicable.

References

- [1] Tian H, Yang J, Xie Z, Liu J. Gliquidone alleviates diabetic nephropathy by inhibiting notch/snail signaling pathway. *Cell Physiol Biochem* 2018;51(5):2085–97.
- [2] Loeffler I, Wolf G. Epithelial-to-Mesenchymal transition in diabetic nephropathy: fact or fiction? *Cells* 2015;4(4):631–52.
- [3] Liang G, Song L, Chen Z, Qian Y, Xie J, Zhao L, et al. Fibroblast growth factor 1 ameliorates diabetic nephropathy by an anti-inflammatory mechanism. *Kidney Int* 2018;93(1):95–109.
- [4] Kanasaki K, Taduri G, Koya D. Diabetic nephropathy: the role of inflammation in fibroblast activation and kidney fibrosis. *Front Endocrinol* 2013;4:7.
- [5] Szejder M, Piwkowska A. AMPK signalling: implications for podocyte biology in diabetic nephropathy. *Biol Cell* 2019;111(5):109–20.
- [6] Lasagni L, Lazzeri E, Shankland SJ, Anders HJ, Romagnani P. Podocyte mitosis - a catastrophe. *Curr Mol Med* 2013;13(1):13–23.
- [7] Kim D, Lim S, Park M, Choi J, Kim J, Han H, et al. Ubiquitination-dependent CARM1 degradation facilitates Notch1-mediated podocyte apoptosis in diabetic nephropathy. *Cell Signal* 2014;26(9):1774–82.
- [8] Pal PB, Sinha K, Sil PC. Mangiferin attenuates diabetic nephropathy by inhibiting oxidative stress mediated signaling cascade, TNF α related and mitochondrial dependent apoptotic pathways in streptozotocin-induced diabetic rats. *PLoS One* 2014;9(9):e107220.
- [9] Duran-Salgado MB, Rubio-Guerra AF. Diabetic nephropathy and inflammation. *World J Diabetes* 2014;5(3):393–8.
- [10] Lim AK, Tesch GH. Inflammation in diabetic nephropathy, vol. 2012. *Mediators Inflamm*; 2012, 146154.
- [11] Elmarakby AA, Sullivan JC. Relationship between oxidative stress and inflammatory cytokines in diabetic nephropathy. *Cardiovasc Ther* 2012;30(1):49–59.
- [12] Mitjavila MT, Moreno JJ. The effects of polyphenols on oxidative stress and the arachidonic acid cascade. Implications for the prevention/treatment of high prevalence diseases. *Biochem Pharmacol* 2012;84(9):1113–22.
- [13] Storniolo CE, Roselló-Catafau J, Pintó X, Mitjavila MT, Moreno JJ. Polyphenol fraction of extra virgin olive oil protects against endothelial dysfunction induced by high glucose and free fatty acids through modulation of nitric oxide and endothelin-1. *Redox Biol* 2014;2:971–7.
- [14] Rossanti R, Shono A, Miura K, Hattori M, Yamamura T, Nakanishi K, et al. Molecular assay for an intronic variant in NUP93 that causes steroid resistant nephrotic syndrome. *J Hum Genet* 2019;64(7):673–9.

- [15] Rosti RO, Sotak BN, Bielas SL, Bhat G, Silhavy JL, Aslanger AD, et al. Homozygous mutation in NUP107 leads to microcephaly with steroid-resistant nephrotic condition similar to Galloway-Mowat syndrome. *J Med Genet* 2017;54(6):399–403.
- [16] Braun DA, Sadowski CE, Kohl S, Lovric S, Astrinidis SA, Pabst WL, et al. Mutations in nuclear pore genes NUP93, NUP205 and XPO5 cause steroid-resistant nephrotic syndrome. *Nat Genet* 2016;48(4):457–65.
- [17] Vollmer B, Lorenz M, Moreno-Andrés D, Bodenhöfer M, De Magistris P, Astrinidis SA, et al. Nup153 recruits the nup107-160 complex to the inner nuclear membrane for interphasic nuclear pore complex assembly. *Dev Cell* 2015;33(6):717–28.
- [18] Braun DA, Lovric S, Schapiro D, Schneider R, Marquez J, Asif M, et al. Mutations in multiple components of the nuclear pore complex cause nephrotic syndrome. *J Clin Invest* 2018;128(10):4313–28.
- [19] Wang P, Zhao F, Nie X, Liu J, Yu Z. Knockdown of NUP160 inhibits cell proliferation, induces apoptosis, autophagy and cell migration, and alters the expression and localization of podocyte associated molecules in mouse podocytes. *Gene* 2018;664:12–21.
- [20] Xie J, Yuan Y, Yao G, Chen Z, Yu W, Zhu Q. Nucleoporin 160 (NUP160) inhibition alleviates diabetic nephropathy by activating autophagy. *Bioengineered* 2021;12(1):6390–402.
- [21] Chen G, Yang Z, Huang Z, Zhou Y, Cui Q, Dong D. LncRNADisease: a database for long-non-coding RNA-associated diseases. *Nucleic Acids Res* 2013;41:D983–6 (Database issue).
- [22] Li Y, Xu K, Xu K, Chen S, Cao Y, Zhan H. Roles of identified long noncoding RNA in diabetic nephropathy. *J Diabetes Res* 2019;2019:5383010.
- [23] Zhao W, Zhang Y, Zhang M, Zhi Y, Li X, Liu X. Effects of total glucosides of paeony on acute renal injury following ischemia-reperfusion via the lncRNA HCG18/miR-16-5p/Bcl-2 axis. *Immunobiology* 2022;227(2):152179.
- [24] Mao B, Wang F, Zhang J, Li Q, Ying K. Long non-coding RNA human leucocyte antigen complex group-18 HCG18 (HCG18) promoted cell proliferation and migration in head and neck squamous cell carcinoma through cyclin D1-WNT pathway. *Bioengineered* 2022;13(4):9425–34.
- [25] Li S, Wang X, Wang T, Zhang H, Lu X, Liu L, et al. Identification of the regulatory role of lncRNA HCG18 in myasthenia gravis by integrated bioinformatics and experimental analyses. *J Transl Med* 2021;19(1):468.
- [26] Che M, Gong W, Zhao Y, Liu M. Long noncoding RNA HCG18 inhibits the differentiation of human bone marrow-derived mesenchymal stem cells in osteoporosis by targeting miR-30a-5p/NOTCH1 axis. *Mol Med* 2020;26(1):106.
- [27] Xia Y, Zhang Y, Wang H. Upregulated lncRNA HCG18 in patients with non-alcoholic fatty liver disease and its regulatory effect on insulin resistance. *Diabetes Metab Syndr Obes* 2021;14:4747–56.
- [28] Ren W, Xi G, Li X, Zhao L, Yang K, Fan X, et al. Long non-coding RNA HCG18 promotes M1 macrophage polarization through regulating the miR-146a/ TRAF6 axis, facilitating the progression of diabetic peripheral neuropathy. *Mol Cell Biochem* 2021;476(1):471–82.
- [29] Li JH, Liu S, Zhou H, Qu LH, Yang JH. starBase v2.0: decoding miRNA-ceRNA, miRNA-ncRNA and protein-RNA interaction networks from large-scale CLIP-Seq data. *Nucleic Acids Res* 2014;42:D92–7.
- [30] Gao YX, Yu CA, Lu JH, Gao HM, Li G, Kong W, et al. ADAMTS-7 expression increases in the early stage of angiotensin II-induced renal injury in elderly mice. *Kidney Blood Press Res* 2013;38(1):121–31.
- [31] Wu J, Guan F, Luo W, Yuan ZW, Chen RQ, Gou X, et al. Prelamin A over-expression promotes detrusor calcification/aging in urinary incontinence via prelamin A accumulation. *J Cell Physiol* 2019;234(10):17800–11.
- [32] Huang JS, Chuang CT, Liu MH, Lin SH, Guh JY, Chuang LY. Klotho attenuates high glucose-induced fibronectin and cell hypertrophy via the ERK1/2-p38 kinase signaling pathway in renal interstitial fibroblasts. *Mol Cell Endocrinol* 2014;390(1–2):45–53.
- [33] Park MJ, Kim DI, Lim SK, Choi JH, Han HJ, Yoon KC, et al. High glucose-induced O-GlcNAcylated carbohydrate response element-binding protein (ChREBP) mediates mesangial cell lipogenesis and fibrosis: the possible role in the development of diabetic nephropathy. *J Biol Chem* 2014;289(19):13519–30.
- [34] Allen DA, Yaqoob MM, Harwood SM. Mechanisms of high glucose-induced apoptosis and its relationship to diabetic complications. *J Nutr Biochem* 2005;16(12):705–13.
- [35] Isermann B, Vinnikov IA, Madhusudhan T, Herzog S, Kashif M, Blautzik J, et al. Activated protein C protects against diabetic nephropathy by inhibiting endothelial and podocyte apoptosis. *Nat Med* 2007;13(11):1349–58.
- [36] Armelloni S, Corbelli A, Giardino L, Li M, Ikehata M, Mattinzoli D, et al. Podocytes: recent biomolecular developments. *Biomol Concepts* 2014;5(4):319–30.
- [37] Sancar-Bas S, Gezgin-Oktayoglu S, Bolkent S. Exendin-4 attenuates renal tubular injury by decreasing oxidative stress and inflammation in streptozotocin-induced diabetic mice. *Growth Factors* 2015;33(5–6):419–29.
- [38] Yao T, Zha D, Gao P, Shui H, Wu X. MiR-874 alleviates renal injury and inflammatory response in diabetic nephropathy through targeting toll-like receptor-4. *J Cell Physiol* 2018;234(1):871–9.
- [39] Aguilar C, Mano M, Eulalio A. MicroRNAs at the host-bacteria interface: host defense or bacterial offense. *Trends Microbiol* 2019;27(3):206–18.
- [40] Zhao H, Ma SX, Shang YQ, Zhang HQ, Su W. microRNAs in chronic kidney disease. *Clin Chim Acta* 2019;491:59–65.
- [41] Fries JWU. MicroRNAs as markers to monitor endothelin-1 signalling and potential treatment in renal disease: carcinoma - proteinuric damage - toxicity. *Biol Cell* 2019;111(7):169–86.
- [42] Dewanjee S, Bhattacharjee N. MicroRNA: a new generation therapeutic target in diabetic nephropathy. *Biochem Pharmacol* 2018;155:32–47.
- [43] Wang L, Li H. MiR-770-5p facilitates podocyte apoptosis and inflammation in diabetic nephropathy by targeting TIMP3. *Biosci Rep* 2020;40(4).
- [44] Fu Y, Wang C, Zhang D, Chu X, Zhang Y, Li J. miR-15b-5p ameliorated high glucose-induced podocyte injury through repressing apoptosis, oxidative stress, and inflammatory responses by targeting Sema3A. *J Cell Physiol* 2019;234(11):20869–78.
- [45] Miguel V, Ramos R, García-Bermejo L, Rodríguez-Puyol D, Lamas S. The program of renal fibrogenesis is controlled by microRNAs regulating oxidative metabolism. *Redox Biol* 2020;40:101851.
- [46] Zhao G, Zhang L, Qian D, Sun Y, Liu W. miR-495-3p inhibits the cell proliferation, invasion and migration of osteosarcoma by targeting C1q/TNF-related protein 3. *Oncotargets Ther* 2019;12:6133–43.
- [47] Mutalifu N, Du P, Zhang J, Akbar H, Yan B, Alimu S, et al. Circ_0000215 increases the expression of CXCR2 and promoted the progression of glioma cells by sponging miR-495-3p. *Technol Cancer Res Treat* 2020;19:1533033820957026.
- [48] Salmena L, Poliseno L, Tay Y, Kats L, Pandolfi PP. A ceRNA hypothesis: the Rosetta Stone of a hidden RNA language? *Cell* 2011;146(3):353–8.
- [49] Peng W, Huang S, Shen L, Tang Y, Li H, Shi Y. Long noncoding RNA NON-HSAG053901 promotes diabetic nephropathy via stimulating Egr-1/TGF- β -mediated renal inflammation. *J Cell Physiol* 2019;234(10):18492–503.
- [50] Long B, Wan Y, Zhang S, Lv L. LncRNA XIST protects podocyte from high glucose-induced cell injury in diabetic nephropathy by sponging miR-30 and regulating AVEN expression. *Arch Physiol Biochem* 2020:1–8.